Identification of Significant Impact Factors on Arrival Flight Efficiency within TMA

Anastasia Lemetti, Tatiana Polishchuk and Valentin Polishchuk
Communications and Transport Systems,
Linköping University, Norrköping, Sweden

Raúl Sáez and Xavier Prats
Department of Physics
Technical University of Catalonia (UPC),
Castelldefels, Barcelona, Spain

***Abstract*—An important step towards improving the flight performance within Terminal Maneuvering Area (TMA) is the identification of the factors causing inefficiencies. Without knowing which exact factors have high impact on which performance indicators, it is difficult to identify which areas could be improved. In this work, we quantify the flight efficiency using average additional time in TMA, average time flown level and additional fuel consumption associated with the inefficient flight profiles. We apply statistical learning methods to assess the impact of different weather phenomena on the arrival flight efficiency, taking into account the current traffic situation. We utilize multiple data sources for obtaining both historical flight trajectories and historical weather measurements, which facilitates a comprehensive analysis of the variety of factors influencing TMA performance. We demonstrate our approach by identifying that wind gust and snow had the most significant impact on Stockholm Arlanda airport arrivals in 2018.**

Keywords—TMA Performance; Arrival Flight Efficiency; Continuous Descent Operations; Fuel Consumption; Key Performance Indicators; Weather Impact; Statistical Learning

I. Introduction

TMAs are known to be the spots of high congestion. Due to the lower maneuverability that can be afforded in a TMA, the same number of movements creates higher complexity in TMA in comparison with the en-route. Airport capacity can be reduced considerably by low visibility, strong winds, thunderstorms in the terminal area and runway closures, especially during the high traffic hours of airport operation. The effects of aircraft noise, fuel burn and related pollutant emissions can impact the quality of life in populated areas near the airports.

In this paper, we apply statistical learning tools to analyze the impact of various weather phenomena on several performance metrics, taking into account the current traffic situation in TMA. In particular, we explore the influence of adverse weather on environmental footprint of arrivals to Stockholm Arlanda airport by estimating the additional fuel burn due to weather-induced inefficiencies. In addition to the coarse flight data (like DDR [1]) and weather data measured on a grid with large spacing (like NOAA [2]), typically used in analysis of enroute flights, we employ frequently-sampled traffic data from OpenSky Network [3] and higher-accuracy weather data from ECMWF ERA5 [4]. The use of multiple sources of traffic and weather data enables a comprehensive data analysis within a single framework. Our framework may be used to predict arrival inefficiencies as well as to analyse and implement reliable mitigation strategies.

Roadmap: The rest of the paper is organized as follows. In Section II we review related work on the topic. Section III describes the methodology we use for analysis of the factors influencing performance of Stockholm Arlanda airport arrivals. We present the results of the data analysis in Section IV. Section V concludes the paper and outlines the future work.

II. Related Work

Quantification of the impact of different weather phenomena on airport operation is reflected in many recent research activities. According to the European Commission Network Manager [5], in 2019 airport Air Traffic Flow Management (ATFM) delays (19,704 min/daily) have increased by 6,5% compared to May 2018 which had high delays due to weather and Air Traffic Control (ATC) industrial action. Several recent SESAR projects addressed one of the objectives of the SESAR 2020 Exploratory Research program with the following meteorology-related task: "to enhance meteorological capabilities and their integration into ATM planning processes for improving ATM efficiency". TBO-MET project [6] addresses the problem of analysing and quantifying the effects of meteorological uncertainty in Trajectory Based Operations [7], [8]. The authors considered two types of meteorological uncertainty: wind uncertainty and convective zones (including individual storm cells). Another weather-related project within SESAR, PNOWWA [9] developed methods to support the ATM challenged by winter weather.

Impact of deep convection and thunderstorms is also subject to ongoing research, e.g. Steiner et al. [10], [11] and Song et al. [12] investigated its implication both on the en-route flow management and for terminal area applications. Klein et al. [13] used a high-level airport model to quantify the impact of weather forecast uncertainty on delay costs. Steiner et al. [14] discuss the crucial effect of accurate forecasts of high-impact winter weather for efficient management of airport and airline capacity and highlight the need of data sharing and integrated decision making between stakeholders. Recent works [15], [16] confirmed the relevance and emphasized the

This research is supported by the SESAR Joint Undertaking under the European Union's Horizon 2020 research and innovation programme under grant agreement No 783287. It is also a part of the IFWHEN project supported by the Swedish Transport Agency (Transportstyrelsen) and in-kind participation of LFV.

importance of quantification of the weather impact on airport operation.

Schults et al. [17] used the ATMAP algorithm, published by Eurocontrol's Performance Review Unit (PRU), which transforms the METAR data into the aggregated weather score weighting the different weather factors. They analysed the correlation of the on-time performance of flight operations with the ATMAP score at major European airports. We apply similar approach in combining several weather metrics and the current traffic intensity into one unified impact factor, to analyse its correlation with different TMA performance indicators.

Dalmau et al. [18] considered weather conditions as features of the machine learning models for predicting take-off time for individual flights. They were able to improve by 30% the Estimated Take-Off Time (ETOT) of each individual flight relative to the one provided by the Enhanced Tactical Flow Management System (ETFMS) Flight Data (EFD).

International Civil Aviation Organization (ICAO) proposed a set of Key Performance Indicators (KPIs) to enable analysis of TMA performance [19]: Additional time in TMA and Level-off during descent. EUROCONTROL developed the methodology used by its Performance Review Unit (PRU) for the analysis of VFE during climb and descent [20].

Performance Review Commission of EUROCONTROL made an assessment of ATM in Europe for the year 2018, where among other indicators reviewed air traffic punctuality and vertical flight inefficiency at the top 30 European airports, including Stockholm airport Arlanda [21]. In addition, EUROCONTOL PRU continues working on the development and maintenance of the open access cloud-based data repositories to enable stakeholders to reproduce the performance review results [22], [23]. EUROCONTROL Experimental Center also develops new performance indicators targeting to capture different aspects of flight inefficiencies in TMA [24], [25].

In [26] fuel consumption is evaluated for terminal areas with a Terminal Inefficiency metric based on the variation in terminal area fuel consumed across flights, reported by a major U.S. airline. Using this metric they quantify the additional fuel burn caused by ATM delay and terminal inefficiencies. Furthermore, in [27] and [28], an analysis of fuel savings of the Continuous Descent Operations (CDO) with respect to conventional procedures is analyzed. A reduction in fuel consumption of around 25-40% by flying CDO was reported.

Estimation of the flight inefficiencies in terms of extra fuel burn calculated based on the algorithm proposed in [29] was considered in the scope of APACHE project (a SESAR 2020 exploratory research project) [30], but mostly for en-route flight phase. Later Prats et al. [31] proposed a family of performance indicators to measure fuel inefficiencies. In this work, we apply similar techniques to fuel estimation during the descent phase within TMA.

III. Methodology

This section provides the description of the impact factors and flight performance indicators we use in this study, as well as the statistical learning methods for analysis of the impact of different factors on TMA performance.

A. Impact Factors

In this work we examine the influence of several impact factors, such as traffic intensity, snow, wind gust and other weather phenomena (detailed below) on the arrival flight performance within TMA.

1) Traffic Intensity: Traffic congestion is known to have a significant influence on the flight performance, and we choose to include this factor into the investigation of the sources of performance inefficiencies within TMA. We calculate the number of arriving aircraft during the chosen time period (one day or one hour), normalize, and call it Traffic Intensity for the given period. Note that in this work we consider only arrival traffic, and only the arrival traffic intensity is taken into account.

2) Snow: Flight diversions are common during significant snow events. Snowy weather causes major disturbances in airport operation, resulting in reduced visibility, slippery runway conditions and the necessity to free runway for snow cleaning. We use the number of snow observations per day as a snow metric, as well as snow density measured in $kg \times m^{-3}$.

3) Wind Speed, Wind Gust: A gust or wind is a brief increase in the speed of the wind. Gusts of wind that change direction quickly and abruptly, are the most dangerous wind conditions on takeoff and landing. Difficult wind conditions can influence the ability of the aircraft to keep up CDO. Wind speed can be calculated from zonal and meridional wind components (u and v components). Historical weather databases usually provide the zonal and meridional wind components and wind gust as separate variables, all measured in $m \times s^{-1}$.

4) Visibility: Depending on cloud ceiling and runway visual range the spacing of aircraft on final approach must be increased. Low visibility reduces the runway capacity for landing aircraft. If this happens during a traffic peak hour, it causes major disruptions. We use surface level measurements of visibility expressed in meters.

5) Convective Available Potential Energy (CAPE): CAPE is the energy a parcel of air has for upward motion, measured in joules per kilogram of air ($J \times kg^{-1}$). The higher the CAPE, the faster and higher the air parcel can rise. Most thunderstorms form in moderately unstable conditions (CAPE up to 1000 $J \times kg^{-1}$) but any value greater than 0 $J \times kg^{-1}$ indicates instability and an increasing possibility of thunderstorms and severe straight line winds. Convective weather poses a significant risk to the safe conduct of an aircraft. The operating procedures for most airlines specify to avoid convective areas whenever possible.

6) Total Cloud Cover: Total cloud cover is the fraction of the sky covered by all the visible clouds. The usual unit of measurement of the cloud cover is $okta$, which is a number of eighths of the sky covered in cloud. Ceilings and cloud cover impact both visual (VFR) and instrument flight rules (IFR).

7) Aggregated Impact Factor: We introduce the aggregated impact factor (AIF), a unified condition metric, representing the current weather and traffic situation. We calculate it using the following algorithm. First, we normalize traffic intensity and all the weather metrics calculated with the granularity of one hour (snow depth, wind speed, CAPE, total cloud cover), to fit into the range from 0 to 1, using the following normalization formula $x - x_{min}/x_{max} - x_{min}, \forall$ metric x. Then we sum them up getting as the result values between 0 and 5. Next, we group numeric values into 25 bins, discretizing the results to obtain the unified score. Note that getting the maximum unified score of 25 is impossible because it would mean the simultaneous weather events such are convective weather and snow, for example. As a result, the observed values of the AIF range between 0 and 15, reflecting the combined weather and traffic statistics at Stockholm Arlanda Airport in 2018.

B. Performance Indicators

In order to capture different aspects of the TMA performance we choose the following key performance indicators.

1) ICAO KPIs: We use two KPIs proposed by ICAO [19]: Additional time in terminal airspace and Level-off during descent. The *additional time in TMA ($KPI08$)* is calculated as the difference between the actual transit time and the time according to the flight plan. As stated in [25], it represents the extra time generated by the arrival management and "is a proxy for the level of inefficiency (holding, sequencing) of the inbound traffic flow".

Vertical inefficiencies during the descent phase result from the inability of flights to keep up CDO. This type of operations enables the execution of a flight profile optimized to the operating capability of the aircraft, giving as a result optimal continuous engine-idle descents (without using speed-breaks) that reduce fuel consumption, gaseous emissions and noise nuisance. If the aircraft levels at intermediate altitudes before landing, this descent is considered as vertical inefficient.

For evaluation of VFE we consider $KPI19.2$, the *average time flown in level flight* inside TMA, using the techniques proposed by EUROCONTROL in [20] with small changes. We identify the point of the trajectory in which the aircraft enters the TMA and use it as a starting point for the calculations (instead of the Top of Descent (ToD), which may lie outside of TMA). A level segment is detected when the aircraft is flying with the vertical speed below the certain threshold. We use the value of 300 feet per minute for this threshold, the minimum time duration of the level flight is considered 30 seconds, and these 30 seconds are subtracted from each level duration as suggested in [20].

2) Fuel-Based PI: Fuel-based PIs capture inefficiencies on tactical ATM layer in vertical domain as explained in [31]. The objective is to compare the fuel consumption of CDO trajectories with the actual flown trajectories. Fuel-based performance indicators are calculated using the 4.2 version of the Base of a Aircraft Data (BADA) [32].

Fuel Consumption: The first expression used, known as the Total-Energy Model, equates the rate of work done by forces acting on the aircraft to the rate of increase in potential and kinetic energy, that is:

$$(T - D)V_{TAS} = mg\frac{dh}{dt} + mV_{TAS}\frac{dV_{TAS}}{dt} \tag{1}$$

Here T is the thrust acting parallel to the aircraft velocity vector, D is the aerodynamic drag, m is the aircraft mass, h is the geodetic altitude, g is the gravitational acceleration and V_{TAS} is the true airspeed. D is computed as follows:

$$D = \frac{1}{2} \cdot \delta \cdot p_0 \cdot \kappa \cdot S \cdot M^2 \cdot C_D \tag{2}$$

Here δ is the pressure ratio, p_0 is the standard atmospheric pressure at mean sea level (MSL), κ is the adiabatic index of air, S is the wing reference area, M is the Mach number and C_D is the drag coefficient. BADA proposes equations for computing C_D depending on the aircraft configuration, and modelled as a polynomial of lift coefficient C_L.

Three separate thrust models are proposed in BADA, depending on the engine type: turbofan, turboprop or piston. Each model includes the contribution from all engines and provides the thrust as a function of airspeed, throttle setting and atmospheric conditions. This is the general formula:

$$T = \delta \cdot W_{mref} \cdot C_T \tag{3}$$

Here δ is the pressure ratio, m_{ref} is the reference mass (obtained from the Propulsive Forces Model (PFM)), W_{mref} is the weight force at m_{ref} and C_T is the thrust coefficient, which is a function of Mach number.

For the three engine types, BADA proposes different equations to compute the thrust coefficient C_T depending on the engine rating: maximum climb, maximum cruise, idle and no rating (direct throttle parameter input). For estimation of the fuel consumption, BADA proposes once again a different model depending on the engine type, and also depending on the engine rating. Each model includes the contribution from all engines and provides the fuel consumption as a function of airspeed, throttle parameter and atmospheric conditions. The general formula for the fuel consumption, F, is:

$$F = \delta \cdot \theta^{\frac{1}{2}} \cdot W_{mref} \cdot a_0 \cdot L_{HV}^{-1} \cdot C_F \tag{4}$$

Here δ is the pressure ratio, θ is the temperature ratio, a_0 is the speed of sound at MSL in standard atmosphere, L_{HV} is the fuel lower heating value (obtained from the PFM) and C_F is the fuel coefficient, which depends on thrust for non-idle ratings. For each aircraft model, BADA provides an xml file with the corresponding aircraft performance data. For instance, the coefficients used to compute the thrust coefficient C_T of the thrust equation (3) are in this file. With the equations stated above, and the xml files for each aircraft, it is possible to compute the fuel consumption of a trajectory. Firts, the thrust is computed. If the aircraft is climbing, max climb rating is chosen and the corresponding thrust formula (depending on

the engine type) is applied. If the aircraft is descending, an idle rating is assumed. In level-offs, the total-energy model (equation (1)) is used in order to compute the corresponding aircraft thrust (drag is computed previously with equation (2)). Then, for non-idle ratings, the thrust computed in the previous step is used to obtain the fuel coefficient C_F used in equation (4). In this way, fuel consumption is obtained. For descents, idle rating is assumed.

Wind was obtained from historical weather data (detailed in subsection IV-A). Furthermore, a 90% of the maximum landing mass has been assumed at the destination airport for all aircraft.

Generation of CDO trajectories: In order to generate the CDO trajectories an optimal control problem has to be solved as explained in details in [33]. First, a state vector with the initial conditions is needed. In this paper, it has been chosen as $x = [v, h, s]$, where v is the true airspeed, h - the altitude of the aircraft, and s - the distance to go. In order to obtain environmentally friendly trajectories, idle thrust is assumed and speed-brakes use is not allowed throughout the descent. In such conditions, the flight path angle is the only control variable in this problem ($u = [\gamma]$), which is used to manage the energy of the aircraft and achieve different times of arrival at the metering fix with minimum fuel consumption and noise nuisance.

The dynamics of x are expressed by the following set of ordinary differential equations, considering a point-mass representation of the aircraft reduced to a "gamma-command" model, where vertical equilibrium is assumed (lift balances weight). In addition, the cross and vertical components of the wind are neglected, and the aerodynamic flight path angle is assumed to be small (i.e.,$\sin\gamma \simeq \gamma$ and $\cos\gamma \simeq 1$):

$$f = \begin{bmatrix} \dot{v} \\ \dot{h} \\ \dot{s} \end{bmatrix} = \begin{bmatrix} \frac{T_{idle} - D}{m} - g\gamma \\ v\gamma \\ v + w \end{bmatrix} \tag{5}$$

where $T_{idle} : \mathbb{R}^{n_x} \to \mathbb{R}$ is the idle thrust; $D : \mathbb{R}^{n_x \times n_u} \to \mathbb{R}$ is the aerodynamic drag; g is the gravity acceleration; w is the wind and m - the mass, which is assumed to be constant because the fuel consumption during an idle descent is a small fraction of the total m [34]. The longitudinal component of the wind $w : \mathbb{R} \to \mathbb{R}$ is modelled by a smoothing spline [35]:

$$w(h) = \sum_{i=1}^{n_c} c_i B_i(h) \tag{6}$$

B_i, $i = 1, \ldots, n_c$, are the B-spline basis functions and $c = [c_1, \ldots, c_{n_c}]$ are control points of the smoothing spline. It should be noted that the longitudinal wind has been modelled as a function of the altitude only, as done in similar works [36]. The control points of the spline approximating the longitudinal wind profile are obtained by fitting historical weather data (detailed in section IV-A).

In this paper, the trajectory is divided in two phases: the latter part of the cruise phase prior the ToD, and the idle descent down to the metering fix. Assuming that the original cruise speed will not be modified after the optimization process, the two-phases optimal control problem can be converted into a single-phase optimal control problem as follows:

$$J_a = \int_{t_0}^{t_f} -\left(\frac{f + \text{CI}}{v_{cr}}\right)(v + w) + f_{idle} + \text{CI}\; dt \tag{7}$$

where $f : \mathbb{R}^{n_x \times n_u} \to \mathbb{R}$ and $f_{idle} : \mathbb{R}^{n_x} \to \mathbb{R}$ are the nominal and idle fuel flow, respectively; and CI is the cost index, which is a parameter chosen by the airspace user that reflects the relative importance of the cost of time with respect to fuel costs [37]. The CI is estimated by assuming that the aircraft was flying at the optimal speed in the cruise phase, as shown in [38].

To generate the optimum trajectories, five input parameters are used: aircraft model, cruise altitude, distance to go (i.e., the distance remaining to the metering fix by following a given route), speed (i.e., the true airspeed of the aircraft in cruise), and the cost index.

C. Backward Selection Method

We aim at identifying the factors with high influence on the chosen PIs. We study this problem using statistical analysis, and the problem is an inference task.

When inference is the goal, there are clear advantages of using simple and relatively inflexible statistical learning methods, such as linear regression. We use multiple linear regression and the method of Backward Selection to determine the statistically significant metrics [39]. The R^2 value for inference tasks can be relatively small, especially when the dependent variable might be greatly affected by other factors (departure traffic intensity, not considered weather phenomena, human factors).

More important than the R^2 value for inference regression analysis is the calculation of $t\text{-}statistics$ and associated $p\text{-}values$. We test whether the discovered dependence could be just a random artefact, i.e., we perform the statistical test on the null-hypothesis H_0 "There is no dependence (regression coefficient is equal to 0), between the PI and the impact factor and the observed value of the regression coefficient can be attributed to pure noise". The small value of associated $p\text{-}value$ (the probability of obtaining the regression coefficient larger than ours, assuming the true value is 0), that is the probability of H_0 being true, indicates that we can reject the hypothesis and justifies the statistical significance of our claim that PI depends on the corresponding impact factor.

On each step of the Backward Selection algorithm we check $F\text{-}statistic$ (the hypothesis test for the the null-hypothesis H_0 "All regression coefficients are equal to 0") and $p\text{-}value$ associated with it. If there is no relationship between the PI and impact factors, we would expect the $F\text{-}statistic$ to take on a value close to 1 [39]. As a cutoff for $p\text{-}value$ we take a typically used 0.05 value. To remove outliers we cap the data at 95-percentile and 5-percentile for the considered PI.

IV. Experimental Results

This section describes the data used in this work and presents the results of the comprehensive analysis of weather on arrival flight performance for the Stockholm Arlanda airport in the year 2018.

A. Data

In this work we use multiple sources of historical data related to the Stockholm Arlanda airport performance.

1) Historical Flight Trajectories: Flight plans are obtained from the Demand Data Repository (DDR2 [1], m1 file format) hosted by EUROCONTROL. For the historical flight trajectories we use DDR2 (m3 file format) and the Historical Database of the OpenSky Network [3], [40].

2) Aircraft Performance Data: Aircraft performance parameters for CDO trajectory generation and fuel consumption calculation are inputed from BADA 4.2 [32]. In the case the aircraft model does not correspond to any of the BADA models, a comparable aircraft in terms of performance and dimensions is used.

3) Historical Weather: Current weather conditions are usually recorded at each airport in the form of METARs. Current and historical METAR data is accessible at different publicly available web sources, e.g. [41]. In addition to information about the location, the day of the month and the UTC time, the METAR contains information about wind, visibility, precipitation, clouding, temperature, and pressure that are relevant for the air traffic, especially for the airport operations. Besides this general weather information, some additional measurements were available related to adverse weather situations, such as information about wind gusts, runway conditions (e.g., ice layer) and thunderstorm related clouds, as well as calculated values of the Runway Visual Range (RVR).

We use snow observation values from the METAR data and calculate how many times per day we observed snow. The observations are conducted every half an hour (48 times per day), so the resulting snow metric can take values from 0 to 48.

Another source of the historical weather data is NOAA [2]. Gridded binary (GRIB) formatted files with $0.5°$ granularity provided by the global forecast system (GFS) of NOAA are used in order to generate the longitudinal wind profiles as a function of the altitude (needed for the trajectory optimization). We also take surface level measurements of visibility, wind gust and CAPE average per day as weather metrics within TMA from the NOAA database to perform regression analysis on daily base.

The ECMWF ERA5 reanalysis dataset provided via the C3S Data Store in form of NetCDF files [4] has an hour time granularity and the data cover the Earth on a $0.25°$ grid. From ECMWF ERA5 dataset we take snow density, u-component and v-component of wind, CAPE and total cloud cover metrics for hourly analysis.

While using various data sources within one framework, we compare and evaluate their applicability for different calculations inside TMA. For example, better data granularity of Opensky Network data makes it a better option to estimate fuel consumption and vertical efficiency inside TMA. While DDR usually provides only 10 to 15 waypoints inside TMA, in Opensky states there are about 800-1000 points, which provide accurate aircraft positions reported every second. However, there are also some errors in the Opensky data, obtained from the transponders. In some trajectories there are repeated waypoints and infeasible time stamps, even with the time advancing (which would mean the aircraft remains still, which is not possible). There are other situations where the latitude and longitude do not seem to correspond to the trajectory we are dealing with, and some of the speed values that could be extracted from Opensky data are wrong too. Another drawback of the OpenSky data is the lack of flight identifier, and aircraft type information, needed for the calculation of fuel consumption. We resolved this problem by merging the data with DDR flight plans (SO6 m1 files).

A more detailed comparison of the data sources was reported in [42]. In general, we recommend Opensky states vectors as a valuable data source for research with high accuracy demand, which however requires sufficient computational resources. On the other hand, due to incompleteness of the Opensky data, DDR2 is better suitable for delay statistics and calculation of the average additional time in TMA.

B. Implementation

We developed a flexible interactive web-based tool to facilitate comprehensive data analysis using different data sources combined into a single framework. The interface implementation is based on the web framework Flask using Python. The data from Opensky network is preliminarily downloaded with the separate Python scripts using OpenSky REST API and SSH agent to access Opensky Impala Shell.

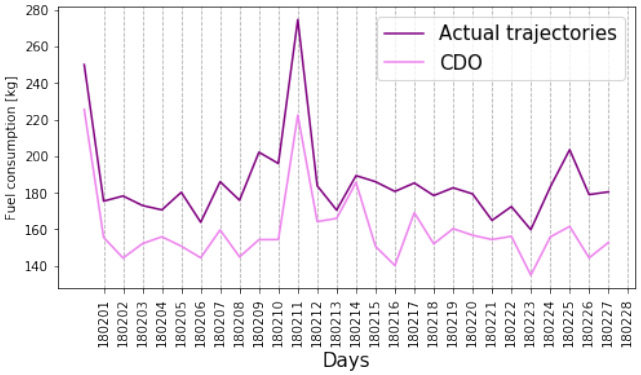

Fig. 1. Average fuel consumption over the flights per day (in kg) for actual flown trajectories and CDO within TMA for arrival flights in Stockholm Arlanda during the month of February 2018.

C. PIs Calculation

1) Additional Time in TMA: For calculation of this PI we compare the flight plans obtained from DDR2 repository (m1 format) against the actual trajectories reported in DDR2 (m3 format) and evaluate the difference in time aircraft spend inside TMA. We use different granularity for calculation of this PI: per hour and per day for the whole year 2018.

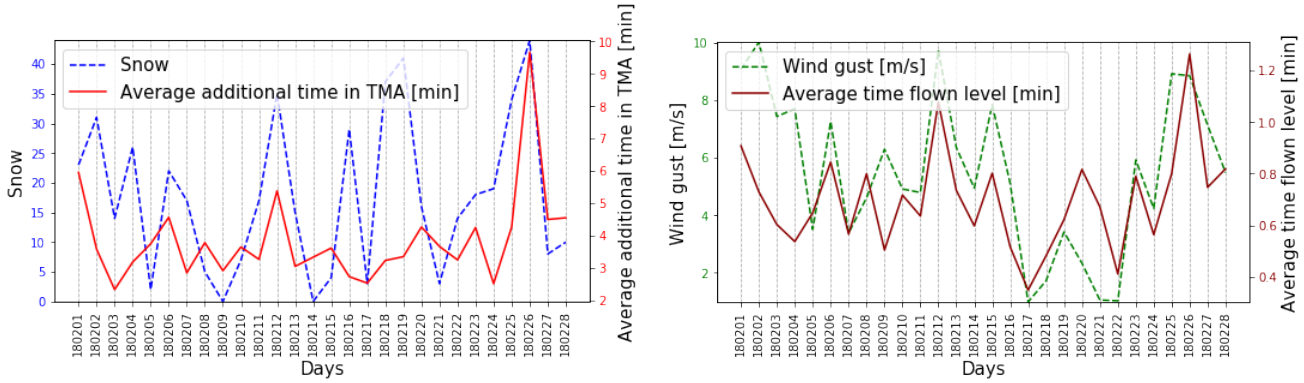

Fig. 2. Weather metrics (snow and wind gust) and PIs (average additional time in TMA and average time flown level) for the month of February 2018.

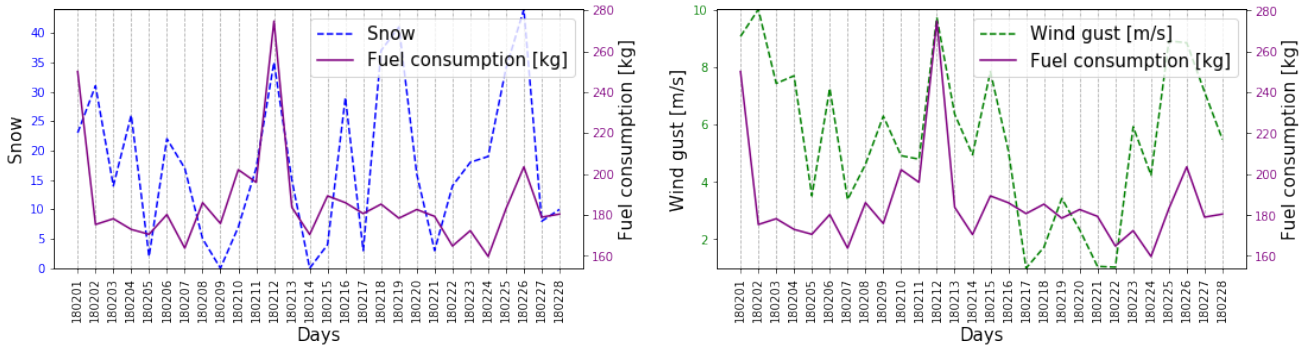

Fig. 3. Weather metrics (snow and wind gust) and the Fuel PI for the month of February 2018.

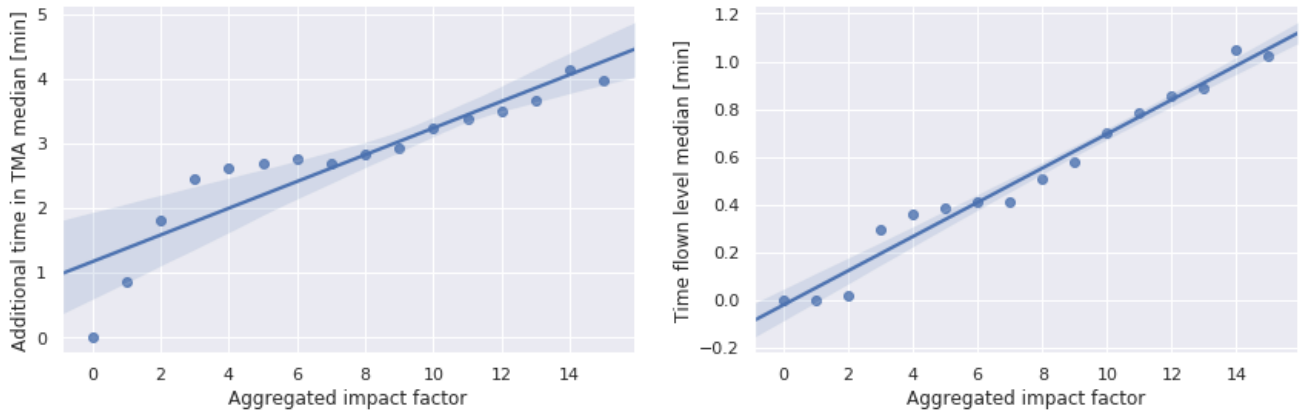

Fig. 4. Regression of flights additional time in TMA and time flown level median values onto the AIF ($R^2 = 0.83$ and $R^2 = 0.97$).

2) Average Time Flown Level: For evaluation of the vertical inefficiency we use OpenSky states data, which provides very accurate levels in aircraft descent. We average the time on levels over one hour and over one day for the whole year 2018.

3) Fuel-based PI: We evaluate the fuel efficiency during the month of February 2018. For calculation of the additional fuel burn inside TMA we compare the fuel consumption of CDO trajectories with the actual flown trajectories. For actual trajectories we use OpenSky Network states data, which provides very accurate aircraft positions with the updates for each second. For CDO calculation the distance to go was also obtained from Opensky Network data.

Absolute values for the fuel consumption are shown in Figure 1, representing the average fuel consumption over the flights per day in February 2018. CDO provide a reduction in fuel consumption, from around a 5% up to a 30% depending on the day, which constitutes a significant fuel inefficiency. It is important to recall that we calculate the fuel inside TMA only; if the whole descent was compared, the difference would

have been lower, as level-offs at lower altitudes are more detrimental for efficiency than those at higher altitudes.

Calculation of the fuel consumption requires the data of high granularity and is a computationally expensive task (for one trajectory the computation takes about 2 minutes of computer time, which for the typical traffic of 300 flights per day, results in about 2 weeks of computation for calculating the fuel for one month.) This was the reason why we calculated this PI only for one month in 2018 (the motivation of choosing February was that there were observed strong winds and several snow events during this month, which is important for evaluation of the impact of weather on fuel consumption presented later in this paper). In future work we consider utilizing more powerful computer resources to continue investigations of the most significant factors influencing fuel efficiency.

D. Analysis of the Influence of Weather and Flight Intensity on TMA Performance

First, to examine the dependency between our performance indicators and different weather phenomena we plot the PI–weather pairs for all days of the year 2018. We observe that not always but often the increase in the weather metric is accompanied by the increase in the corresponding PI (e.g. February 12 and 26 in Figure 2, February 1, 12 and 26 in Figure 3). This supports the assumptions that there is some correlation between weather conditions and flight efficiency within TMA, which we will study using statistical learning methods further on.

1) PIs vs AIF: Next, we analyse the influence of our impact factors aggregated into the AIF (described in Section III-A7) on our PIs inside TMA. The resulting AIF values are calculated per hour. After discretization each AIF value falls into the corresponding bin ranging from 0 to 15. For each flight we calculate additional time in TMA, time flown level and assign an AIF value (AIF of the closest to arrival time hour). We perform the regression of the additional time in TMA and the time flown level medians per bin onto AIF values. The mean values can not be taken here because of the high deviations of PIs inside bins. We got the strong correlation between the PIs medians and the AIF with $R^2 = 0.83$ for additional time in TMA and $R^2 = 0.97$ for time flown level, illustrated in Figures 4.

Unfortunately, similar analysis for the fuel-based PI is not possible here due to the absence of fuel calculations for the whole year. Future work aims to fill in this gap.

2) Additional Time in TMA vs Individual Impact Factors: After proving the combination of the chosen impact factors has a noticeable impact on the chosen PIs, we identify which of the individual factors have higher influence on each PI separately.

We apply Backward Selection method for regressing the average additional time in TMA onto normalized weather metrics and traffic intensity. Three steps of the Backward Selection are summarized in Table I. We identify traffic intensity, snow and wind gust as the most significant factors for average additional time in TMA.

3) Average Time Flown Level vs Individual Impact Factors: Next, we perform regression analysis of the average time flown level on individual impact factors. Here the average PI values are calculated per hour and weather data is taken from an alternative data source, i.e. the ECMWF ERA5 [4] with the hourly granularity. The weather metrics considered are snow density, wind speed, CAPE and total cloud cover. We also take the traffic intensity into account. Two steps of the Backward Selection algorithm are presented in Table II. We identify only CAPE as an insignificant metric (with the $p - value = 0.93$). The other individual factors have significant influence on the vertical efficiency PI, and together with the traffic intensity, snow and wind speed reveal strong influence, and hence, can be identified as the most important.

4) Fuel PI vs Individual Impact Factors: Similarly, we regress the average per day additional fuel consumption for the month of February, 2018 onto the weather data from NOAA [2] for the same month. The steps of the Backward Selection algorithm are presented in Table III. Only wind gust is identified as a significant factor influencing additional fuel consumption within TMA. All the other factors with the corresponding higher $p-values$ were disregarded on the four steps of the algorithm.

V. Conclusions and Future Work

This work is a step towards understanding the causes of flight inefficiencies inside TMA and the impact of weather on different aspects of TMA performance. Our results show that wind gust and snow are the factors with the most significant impact on the majority of our KPIs. Since convective weather is relatively rare event in our study area, our conclusion that CAPE alone does not fully reveal the influence of convective weather on inefficiencies within TMA may be of limited applicability. Future work may explore better descriptors of convective weather intensity which include more environmental variables, as well as cloud ceiling metrics for evaluation of visibility. In particular, we target integration of the advanced weather prediction methodologies, developed within the related SESAR projects (e.g. [6], [9]), into the evaluation and subsequent optimization of route planning within TMA.

References

[1] EUROCONTROL, *DDR2 Ref. Manual for General Users 2.9.4*, 2017.

[2] "National Oceanic and Atmospheric Administration (NOAA)," https://www.ncdc.noaa.gov/data-access/model-data/model-datasets/global-forcast-system-gfs, last accessed 20.01.2020.

[3] "OpenSky Network," https://opensky-network.org, accessed 20.01.2020.

[4] "European Centre for Medium-Range Weather Forecasts (ECMWF) provided via Copernicus Climate Change Service (C3S) Data Store," https://cds.climate.copernicus.eu, last accessed 20.01.2020.

[5] "European Commision Network Manager. Monthly Network Operations Report," May 2019.

[6] "Meteorological Uncertainty Management for Trajectory Based Operations," https://tbomet-h2020.com/, last accessed 29.09.2019.

[7] E. Hernández, A. Valenzuela, and D. Rivas, "Probabilistic aircraft conflict detection considering ensemble weather forecast," *SID'16*.

[8] D. Rivas, R. Vazquez, and A. Franco, "Probabilistic analysis of aircraft fuel consumption using ensemble weather forecasts," in *ICRAT'16*.

[9] "Probabilistic Nowcasting of Winter Weather for Airports Horizon 2020 SESAR project, 2016-2018," http://pnowwa.fmi.fi, accessed 05.22.20.

TABLE I
BACKWARD SELECTION ALGORITHM RESULTS FOR MULTIPLE LINEAR REGRESSION OF THE AVERAGE ADDITIONAL TIME IN TMA VERSUS IMPACT FACTORS

R^2_{adj}	$F\text{-}stat.$	$Prob\ (F\text{-}stat.)$	Traffic Intensity		Snow		Visibility		Wind gust		CAPE	
			$coef.$	$p\text{-}value$	$coef.$	$p\text{-}value$	$coef.$	$p\text{-}value$	$coef.$	$p\text{-}value$	$coef.$	$p\text{-}value$
0.18	18.71	7.58e-15	0.9746	0.0	0.9356	0.0	-0.0961	0.551	1.0680	0.0	0.3570	0.347
0.18	20.84	1.83e-15	0.9838	0.0	0.9926	0.0			1.0850	0.0	0.4363	0.22
0.18	27.24	6.65e-16	0.9629	0.0	0.9657	0.0			1.0758	0.0		

TABLE II
BACKWARD SELECTION ALGORITHM RESULTS FOR MULTIPLE LINEAR REGRESSION OF THE AVERAGE TIME FLOWN LEVEL VERSUS IMPACT FACTORS

R^2_{adj}	$F\text{-}stat.$	$Prob\ (F\text{-}stat.)$	Traffic Intensity		Snow density		Total cloud cover		Wind speed		CAPE	
			$coef.$	$p\text{-}value$	$coef.$	$p\text{-}value$	$coef.$	$p\text{-}value$	$coef.$	$p\text{-}value$	$coef.$	$p\text{-}value$
0.16	335.1	0.0	0.9049	0.0	0.1988	0.0	0.0861	0.0	0.4379	0.0	0.0120	0.903
0.16	418.9	0.0	0.9049	0.0	0.1982	0.0	0.0862	0.0	0.4376	0.0		

TABLE III
BACKWARD SELECTION ALGORITHM RESULTS FOR MULTIPLE LINEAR REGRESSION OF THE AVERAGE ADDITIONAL FUEL CONSUMPTION VERSUS IMPACT FACTORS

R^2_{adj}	$F\text{-}stat.$	$Prob\ (F\text{-}stat.)$	Traffic Intensity		Snow		Visibility		Wind gust		CAPE	
			$coef.$	$p\text{-}value$	$coef.$	$p\text{-}value$	$coef.$	$p\text{-}value$	$coef.$	$p\text{-}value$	$coef.$	$p\text{-}value$
0.12	1.720	0.172	6.1601	0.802	25.7167	0.206	13.3889	0.357	61.3318	0.044	-448.104	0.761
0.15	2.225	0.0978			25.1084	0.203	13.0228	0.358	61.4745	0.039	-398.98	0.780
0.18	3.057	0.0477			25.2038	0.192	14.1696	0.287	60.2592	0.037		
0.18	3.963	0.0320			15.4873	0.360			58.7683	0.042		
0.18	7.092	0.0131							67.8743	0.013		

[10] M. Steiner, R. Bateman, D. Megenhardt, Y. Liu, M. Xu, M. Pocernich, and J. Krozel, "Translation of ensemble weather forecasts into probabilistic air traffic capacity impact," *Air Traffic Control Quarterly*, vol. 18, no. 3, pp. 229–254, 2010.

[11] M. Steiner, W. Deierling, K. Ikeda, E. Nelson, and R. Bass, "Airline and airport operations under lightning threats-safety risks, impacts, uncertainties, and how to deal with them all," in *6th AIAA Atmospheric and Space Environments Conference*, 2014, p. 2900.

[12] L. Song, D. Greenbaum, and C. Wanke, "The impact of severe weather on sector capacity," in *ATM Seminar*, 2009.

[13] A. Klein, S. Kavoussi, and R. S. Lee, "Weather forecast accuracy: Study of impact on airport capacity and estimation of avoidable costs," in *ATM Seminar*, 2009.

[14] M. Steiner, "Coping with adverse winter weather: emerging capabilities in support of airport and airline operations," *Journal of Air Traffic Control*, 2015.

[15] S. Reitmann, S. Alam, and M. Schultz, "Advanced quantification of weather impact on air traffic management," in *ATM Seminar*, 2019.

[16] M. Steinheimer, C. Kern, and M. Kerschbaum, "Quantification of weather impact on air arrival management," in *ATM Seminar*, 2019.

[17] M. Schultz, S. Lorenz, R. Schmitz, and L. Delgado, "Weather impact on airport performance," *Aerospace*, vol. 5, no. 4, p. 109, 2018.

[18] R. Dalmau, F. Ballerini, H. Naessens, S. Belkoura, and S. Wangnick, "Improving the predictability of take-off times with machine learning."

[19] "KPI Overview," https://www4.icao.int/ganpportal/ASBU/KPI, last accessed 20.01.2020.

[20] EUROCONTROL, "Analysis of vertical flight efficiency during climb and descent," 2017.

[21] "EUROCONTROL, Performance Review Report: An Assessment of Air Traffic Management in Europe during the Calendar Year 2018."

[22] E. Spinielli, R. Koelle, M. Zanin, and S. Belkoura, "Initial Implementation of Reference Trajectories for Performance Review," in *SIDs*, 2017.

[23] E. Spinielli, R. Koelle, K. Barker, and N. Korbey, "Open Flight Trajectories for Reproducible ANS Performance Review," in *SIDs*, 2018.

[24] R. Christien, E. Hoffman, and K. Zeghal, "Spacing and pressure to characterise arrival sequencing," in *ATM Seminar*, 2019.

[25] P. Pasutto, E. Hoffman, and K. Zeghal, "Vertical efficiency in descent compared to best local practices," in *ATM Seminar*, 2019.

[26] M. S. Ryerson, M. Hansen, and J. Bonn, "Time to burn: Flight delay, terminal efficiency, and fuel consumption in the national airspace system," *Transportation Research Part A: Policy and Practice*, vol. 69, pp. 286–298, 2014.

[27] H. Fricke, C. Seiss, and R. Herrmann, "Fuel and energy benchmark analysis of continuous descent operations," in *ATM Seminar*, 2015.

[28] F. Wubben and J. Busink, "Environmental Benefits of continuous descent approaches at Schiphol airport compared with conventional approach procedures," National Aerospace Laboratory, Tech. Rep., 2000.

[29] G. B. Chatterji, "Fuel burn estimation using real track data," in *ATIO'11*, 2011, p. 6881.

[30] X. Prats, I. Agüi, F. Netjasov, G. Pavlovic, and A. Vidosavljevic, "APACHE-Final project results report," 2018.

[31] X. Prats, R. Dalmau, and C. Barrado, "Identifying the sources of flight inefficiency from historical aircraft trajectories," in *ATM Seminar*, 2019.

[32] EUROCONTROL, "User Manual for the Base of Aircraft Data (BADA) Family 4," 2014.

[33] R. Sáez, X. Prats, T. Polishchuk, V. Polishchuk, and C. Schmidt, "Automation for Separation with CDOs: Dynamic Aircraft Arrival Routes," in *ATM Seminar*, 2019.

[34] J. P. Clarke, N. T. Ho, L. Ren, J. Brown, K. Elmer, K. F. Zou, C. Hunting, D. McGregor, B. Shivashankara, K. Tong, A. W. Warren, and J. Wat, "Continuous descent approach: Design and flight test for Louisville international airport," *J. of Aircraft*, vol. 41, no. 5, pp. 1054–1066, 2004.

[35] C. de Boor, "On calculating with B-splines," *Journal of Approximation Theory*, vol. 6, no. 1, pp. 50–62, 1972.

[36] P. M. A. de Jong, J. J. van der Laan, A. C. Veld, M. M. van Paassen, and M. Mulder, "Wind-Profile Estimation Using Airborne Sensors," *Journal of Aircraft*, vol. 51, no. 6, pp. 1852–1863, 2014.

[37] Airbus, "Getting to grips with the cost index - Issue II," Tech. Rep. 2, 1998.

[38] R. Sáez, R. Dalmau, and X. Prats, "Optimal assignment of 4D close-loop instructions to enable CDOs in dense TMAs," in *DASC*, 2018.

[39] G. James, D. Witten, T. Hastie, and R. Tibshirani, *An Introduction to Statistical Learning: with Applications in R*. Springer, 2017.

[40] M. Schäfer, M. Strohmeier, V. Lenders, I. Martinovic, and M. Wilhelm, "Bringing Up OpenSky: A Large-scale ADS-B Sensor Network for Research," in *IPSN'14*, 2014.

[41] "Meteorological Aviation Routine Weather Reports (METAR)," https://mesonet.agron.iastate.edu/, last accessed 20.01.2020.

[42] T. Polishchuk, A. Lemetti, and R. Saez, "Evaluation of Flight Efficiency for Stockholm Arlanda Airport using OpenSky Network Data," in *OpenSky Workshop 2019*, ser. EPiC Series in Computing, vol. 67, pp. 13–24. [Online]. Available: https://easychair.org/publications/paper/hk2Q